

## Synthesis, Characterization and Antibacterial Activities of SnO<sub>2</sub>-Fe<sub>3</sub>O<sub>4</sub> Nanocomposites

Widya Twiny Rizki<sup>1</sup>, Poedji Loekitowati Hariani<sup>2,3</sup>, Addy Rachmat<sup>2,3</sup>, Muhammad Said<sup>2,3</sup> and Nur Hanis Hayati Hairom<sup>3</sup>

<sup>1</sup>Magister Program of Chemistry, Faculty of Mathematics and Natural Sciences, Sriwijaya University, Jalan Padang Selasa, Palembang, Indonesia

<sup>2</sup>Department of Chemistry, Faculty of Mathematics and Natural Sciences, Sriwijaya University, Jalan Palembang-Prabumulih, Indralaya, Indonesia

<sup>3</sup>Research Centre of Advanced Material and Nanocomposite, Faculty of Mathematics and Natural Sciences, Sriwijaya University, Jalan Palembang-Prabumulih, Indralaya, Indonesia

<sup>4</sup>Jabatan Teknologi Kejuruteraan Kimia, Fakulti Teknologi Kejuruteraan, Universiti Tun Hussein Onn Malaysia, 86400 Parit Raja, Johor, Malaysia

\*Corresponding Author: [widyatwinirizki@gmail.com](mailto:widyatwinirizki@gmail.com)

### Abstract

Synthesis SnO<sub>2</sub>-Fe<sub>3</sub>O<sub>4</sub> nanocomposite using the hydrothermal method was conducted. The purpose of this study was to determine the best mass ratio in the synthesis of SnO<sub>2</sub>-Fe<sub>3</sub>O<sub>4</sub>. Nanocomposite SnO<sub>2</sub>-Fe<sub>3</sub>O<sub>4</sub> were made with mass ratio (1:1), (1:2) and (2:1) were characterized using XRD and FTIR. The result of SnO<sub>2</sub> characterization using XRD analysis showed a sharp intensity peak at  $2\theta = 26.5$ . The result of Fe<sub>3</sub>O<sub>4</sub> XRD analysis showed a sharp intensity peak at  $2\theta = 35.86$ . The XRD characterization result of SnO<sub>2</sub>-Fe<sub>3</sub>O<sub>4</sub> (1:2)  $2\theta = 26.74$  and  $34.08$ . Based on the XRD characterization, it can be concluded the best mass ratio for SnO<sub>2</sub>-Fe<sub>3</sub>O<sub>4</sub> was (1:2). FTIR spectra shows nanocomposite SnO<sub>2</sub>-Fe<sub>3</sub>O<sub>4</sub> absorption band at  $590\text{ cm}^{-1}$  is a characteristic peak of Sn-O and peak at  $563\text{ cm}^{-1}$  corresponds to Fe-O. The result of TEM depicted morphology in the shape of a rod that has a flat hexagonal crystallographic plane and has a structure in the form of aggregation. Based on the observation result of the antibacterial test, SnO<sub>2</sub>-Fe<sub>3</sub>O<sub>4</sub> nanocomposite has antibacterial properties that the inhibition zone against *Staphylococcus aureus* is better than *Escherichia coli*.

**Keywords:** Nanocomposite, magnetite particle, hydrothermal, *Staphylococcus aureus*, *Escherichia coli*.

### Abstrak (Indonesian)

Sintesis nanokomposit SnO<sub>2</sub>-Fe<sub>3</sub>O<sub>4</sub> dengan metode hidrotermal telah dilakukan. Tujuan dari penelitian ini untuk mengetahui perbandingan massa terbaik. Nanokomposit SnO<sub>2</sub>-Fe<sub>3</sub>O<sub>4</sub> disintesis dengan perbandingan massa (1:1), (1:2) dan (2:1) dan dikarakterisasi menggunakan XRD dan FTIR. Difraktogram SnO<sub>2</sub> menunjukkan intensitas tertinggi pada sudut  $2\theta = 26,5$ . Fe<sub>3</sub>O<sub>4</sub> menunjukkan pola difraksi dengan intensitas tertinggi pada sudut  $2\theta = 35,86$ . Hasil karakterisasi SnO<sub>2</sub>-Fe<sub>3</sub>O<sub>4</sub> menunjukkan pola difraktogram dengan intensitas tertinggi pada sudut  $2\theta = 26,74$  and  $34,08$  dengan intensitas puncak menurun dengan semakin banyaknya Sn. Hasil karakterisasi SnO<sub>2</sub>-Fe<sub>3</sub>O<sub>4</sub> menggunakan FTIR menunjukkan terjadinya pita penyerapan pada  $590\text{ cm}^{-1}$  yang merupakan puncak karakteristik dari Sn-O dan pita penyerapan pada  $563\text{ cm}^{-1}$  yang sesuai dengan Fe-O. Citra TEM memperlihatkan morfologi material berupa batang yang memiliki bidang kristalografi heksagonal datar dan memiliki struktur berupa agregasi. Berdasarkan hasil pengamatan uji antibakteri, nanokomposit SnO<sub>2</sub>-Fe<sub>3</sub>O<sub>4</sub> memiliki sifat antibakteri dimana zona hambat terhadap *Staphylococcus aureus* lebih baik daripada *Escherichia coli*.

**Kata Kunci:** Nanokomposit, partikel magnetik, hidrotermal, *Staphylococcus aureus*, *Escherichia coli*.

### Article Info

Received 15 September 2020  
Received in revised 1  
October 2020  
Accepted 5 October 2020  
Available online 20 October  
2020

## INTRODUCTION

Wu [1] reported that SnO<sub>2</sub> has photocatalytic ability to degrade dyes and other organic compounds. The photocatalysts capability of a semiconductor can be improved using modification, including using doping, the development of composites which include semiconductors, semiconductors-metal, and semi-conductor-non-metals. [2] stated that Fe<sub>3</sub>O<sub>4</sub> nonmagnetic material is a semiconductor that provides the best effect between photo degradation performance and stability in water media. Research conducted by [3] shows that Fe<sub>3</sub>O<sub>4</sub> can be classified as a semiconductor with a bandgap between 0.3 eV. Fe<sub>3</sub>O<sub>4</sub> has the strongest magnetic properties among other iron oxides.

Several methods used in the synthesis of semiconductor oxide nanoparticles included: the sol-gel method [4], the flame spray method [5], and the hydrothermal method [6]. The hydrothermal method is a method that uses water and heat, which in turn converts the solution into crystals which is carried out in a closed system to prevent the loss of solvent when heated above its boiling point [7]. The hydrothermal method has the advantage of being able to produce higher crystallinity and purity [8]. Research that has been conducted by Wang [9] resulted in the synthesis of making SnO<sub>2</sub>-Fe<sub>3</sub>O<sub>4</sub> using the hydrothermal method. In this study, two methods for the synthesis of SnO<sub>2</sub>-Fe<sub>3</sub>O<sub>4</sub> will be combined, namely the hydrothermal method and the coprecipitation method. By combining the two methods, it is expected that the resulting nanocomposite will have high purity and high magnetic properties.

SnO<sub>2</sub> is a nanoparticle material that has been widely applied as an alternative material in various fields. One of them is in the environmental field with its photocatalytic ability to degrade pollutants. Photocatalyst material can kill both Gram-negative and Gram-positive bacteria [10]. Photocatalyst materials can be used as antibacterial agents for *Staphylococcus aureus* and *Escherichia coli*, this is indicated by the formation of an inhibition zone in the results of the observation.

Based on the description, the synthesis of SnO<sub>2</sub>-Fe<sub>3</sub>O<sub>4</sub> nanocomposite by hydrothermal method with various ratios (1:1, 1:2, and 2:1) will be conducted. The resulting photocatalysts will be characterized using XRD, FTIR and TEM.

## MATERIALS AND METHODS

### Materials

Chemical used were analytical grades i.e. HCl, H<sub>2</sub>SO<sub>4</sub>, H<sub>2</sub>O<sub>2</sub>, SnCl<sub>2</sub>·2H<sub>2</sub>O, FeCl<sub>3</sub>·6H<sub>2</sub>O, FeCl<sub>2</sub>·4H<sub>2</sub>O, NaOH, NaNO<sub>3</sub>, bacteria *Staphylococcus aureus* and *Escherichia coli*, Nutrient Agar (NA), Nutrient Broth (NB) and aquadest.

### Methods

#### Synthesis SnO<sub>2</sub>

SnCl<sub>2</sub>·2H<sub>2</sub>O 0.9 g dissolved in 50 mL of distilled water and 25 mL of absolute ethanol. The solution was transferred to Teflon and heated hydrothermally in an oven at 150°C for 12 hours. The precipitate was separated using a 10,000-rpm centrifuge, the precipitate washed several times with distilled water and ethanol. The precipitate dried at 70°C for 24 hours and characterized using XRD.

#### Synthesis Fe<sub>3</sub>O<sub>4</sub>

The synthesis was carried out by the method of coprecipitation. Preparation of Fe<sub>3</sub>O<sub>4</sub> by dissolving 1.99 g FeCl<sub>2</sub>·4H<sub>2</sub>O and 5.41 g FeCl<sub>3</sub>·6H<sub>2</sub>O in 100 mL of distilled water. To the mixture, 1 M NaOH was added gradually while stirring until a black precipitate was formed and the pH of the solution was ± 12. The precipitate was separated and dried in an oven at T = 70°C. The precipitate obtained was characterized using XRD.

#### Synthesis SnO<sub>2</sub>-Fe<sub>3</sub>O<sub>4</sub> nanocomposites

The Nanocomposite with the ratio of SnO<sub>2</sub>-Fe<sub>3</sub>O<sub>4</sub> = 1: 1, made by adding 0.88 g Fe<sub>3</sub>O<sub>4</sub> with 50 mL distilled water, 25 mL ethanol and 0.88 g SnO<sub>2</sub>. The mixture was put into Teflon and heated hydrothermal in an oven at a temperature of 150 °C for 12 hours. The precipitate was separated using a 10,000 rpm centrifuge, the precipitate was washed several times with distilled water and ethanol. The precipitate obtained was dried at 70 °C for 24 hours. Nanocomposites were synthesized for other comparisons, namely 1: 2 and 2: 1. The resulting nanocomposites were characterized using XRD, FTIR and TEM.

#### Antibacterial Test

The antibacterial test was carried out using the diffusion disk method. The bacteria used were *Staphylococcus aureus* ATCC 6538 and *Escherichia coli* ATCC 25922. SnO<sub>2</sub>-Fe<sub>3</sub>O<sub>4</sub> nanocomposites were prepared with varying

concentrations (0; 12.5; 25; 50; 100 and 200 µg/mL) using water solvent. Each of the tested bacteria was inserted into a petri dish with Nutrient Agar (NA) media. 10 µL of SnO<sub>2</sub>-Fe<sub>3</sub>O<sub>4</sub> nanocomposites with varying concentrations were implanted into the Petri dishes using 6 mm diameter paper disks. Furthermore, the petri dishes were wrapped with parafilm tape and incubated at 37°C for 24 hours. Antibacterial activity is determined by measuring the inhibitory diameter in millimeters.

#### Data Analysis

Particle size can be determined using Debye Scherer's equation shown in equation 1:

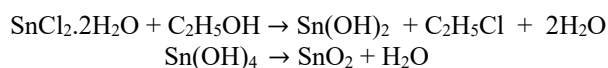
$$d = \frac{0,9\lambda}{FWHM \cos(\theta)} \quad (1)$$

Where d is particle size, λ is the X-ray wavelength, θ is the Bragg angle.

## RESULTS AND DISCUSSION

### Synthesis of SnO<sub>2</sub>

In this research, the synthesis of SnO<sub>2</sub> by the hydrothermal method has been carried out. According to Huda [11] the hydrothermal method has the advantage of being able to produce higher crystallinity. The precursors used in this research were Tin (II) Chloride and used ethanol as a solvent. Synthesis of SnO<sub>2</sub> in this research indicated by the reaction:



Synthesis of SnO<sub>2</sub> in this research indicated by the diffractogram of the obtained phase that is comparable with the standard-issue by Joint Committee on Powder Diffraction (JCPDS) No. 88-0287. The diffractogram is shown in Figure 1.

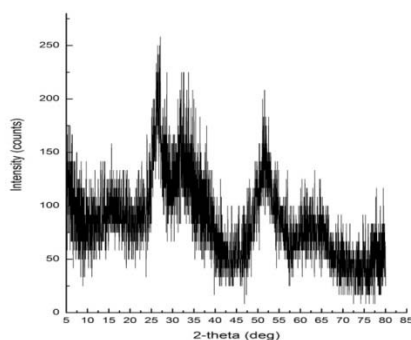


Figure 1. Diffractogram of SnO<sub>2</sub>

Based on Figure 1. shows the diffraction pattern of SnO<sub>2</sub> nanomagnetic X-rays in which the peak widened with the center of peak 2θ = 26.52, 32.1, and 51.8. Data from XRD characterization results and particle size calculations for SnO<sub>2</sub> using the Debye-Scherer formula. From the calculation, the obtained size of SnO<sub>2</sub> 2,829 nm, which shows that SnO<sub>2</sub> has a nanoparticle shape because it has a particle size of below 100 nm [12].

### Synthesis of Magnetite Particle (Fe<sub>3</sub>O<sub>4</sub>)

Magnetite nanoparticles were synthesized using the coprecipitation method. The coprecipitation method is a method of depositing more than a substance together when it passes through the saturation point [13]. The advantages of coprecipitation include a simple method, fast processing and can be used at room temperature. The precursors used in this research were FeCl<sub>2</sub>·4H<sub>2</sub>O and FeCl<sub>3</sub>·6H<sub>2</sub>O. This study uses a strong base of sodium hydroxide as a precipitation agent for the particles to be synthesized. According to Liu [14] The strong base of sodium hydroxide has been chosen because its effectiveness in producing magnetite and the deposition process is faster.

Based on this reaction the formation of magnetite occurs in two stages. The first stage is to homogenize FeCl<sub>3</sub>·6H<sub>2</sub>O and FeCl<sub>2</sub>·4H<sub>2</sub>O. This reaction occurs at the pH of around 2-4 where the stirred solution produces a brownish-orange color. The second stage is adding NaOH by titrating it slowly until the solution forms a black precipitate. The result indicates that magnetite nanoparticles have formed. According to Li [15], magnetite nanoparticle deposits form in the pH range 8-14. The magnetite nanoparticle powder gives a strong magnetic response when it is exposed to a magnet surface as shown in Figure 2. This indicates that the synthesis was successful.



Figure 2. The Magnetite Nanoparticles exposed to the magnets

The synthesized magnetic nanoparticles were characterized using XRD which showed a diffraction angle of  $2\theta$ , peak intensity, and type of phase. Furthermore, it was done by comparing the peaks formed on  $\text{Fe}_3\text{O}_4$  diffractogram with JCPDS data. Based on the standard-issue by Joint Committee on Powder Diffraction (JCPDS) No. 65-30107 there were five characteristics of the peak of  $2\theta$ , namely  $30.205^\circ$ ;  $35.515^\circ$ ;  $43.325^\circ$ ;  $53.711^\circ$ ;  $57.215^\circ$  and  $62.76^\circ$  with field indexes (220), (311), (400), (422), (511), and (440) [16]. The diffractogram results in Figure 3. show that the  $\text{Fe}_3\text{O}_4$  sample analyzed contains sharp peaks at an angle  $30.52^\circ$ ;  $35.86^\circ$ ;  $43.44^\circ$ ;  $53.72^\circ$ ;  $57.2^\circ$  and  $62.76^\circ$ .

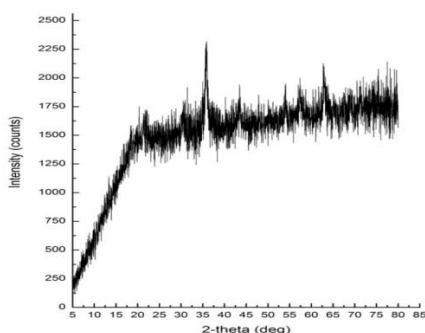


**Figure 3.** XRD pattern of Magnetite Nanoparticles

Based on Figure 3. shows the diffraction pattern of  $\text{Fe}_3\text{O}_4$  nanomagnetic X-rays in which the peak widened with the center of peak  $2\theta = 35.86$  and  $57.2$ . It was found that magnetite has been successfully synthesized. Data from XRD characterization results and particle size calculations for magnetite nanoparticles using the Debye-Scherrer formula. From the calculation, the obtained size of magnetite nanoparticle  $13.66$  nm, which shows that  $\text{Fe}_3\text{O}_4$  has a nanoparticle shape because it has a particle size of below  $100$  nm and the crystal size of  $\text{Fe}_3\text{O}_4$   $122.66$ .

#### Synthesis of $\text{SnO}_2\text{-Fe}_3\text{O}_4$ Nanocomposite and Characterization using XRD

The synthesis of  $\text{SnO}_2\text{-Fe}_3\text{O}_4$  nanocomposite with various mass ratios (1:1), (1:2) dan (2:1) has been carried out using the hydrothermal method. This method was done by mixing  $\text{SnO}_2$  and  $\text{Fe}_3\text{O}_4$  into hydrothermal Teflon. The solvent used in this method were ethanol and water. The dried of  $\text{SnO}_2\text{-Fe}_3\text{O}_4$  composite powder has the same black color as the magnetite nanoparticle. Based on Figure 4. the difference was in the strength of the magnetic attraction response that is weaker than the magnetite

nanoparticle ( $\text{Fe}_3\text{O}_4$ ), due to the addition of Sn to composite [16].

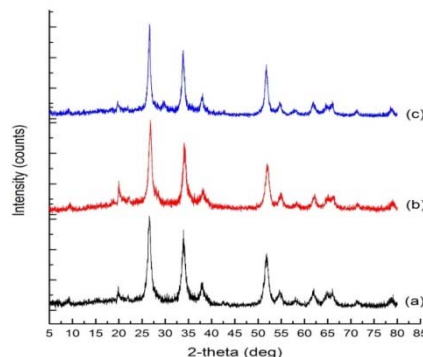


**Figure 4.** XRD patterns of (a)  $\text{SnO}_2\text{-Fe}_3\text{O}_4$  1:1, (b)  $\text{SnO}_2\text{-Fe}_3\text{O}_4$  1:2 and (c)  $\text{SnO}_2\text{-Fe}_3\text{O}_4$  2:1

Based on Figure 4, the  $2\theta$  angle in the  $\text{SnO}_2\text{-Fe}_3\text{O}_4$  (1:1), (1:2), and (2:1) composite has characteristics not much different from the  $2\theta$  angle of  $\text{SnO}_2$  namely at  $26.52^\circ$ . The peak intensity of the  $\text{SnO}_2\text{-Fe}_3\text{O}_4$  composite was seen to decrease with the addition of  $\text{SnO}_2$  into the composite. Based on the research Wang and Yao, 2009 that in the composite comparison the intensity decrease with the  $\text{SnO}_2$  peak covered by the crystallite of magnetite nanoparticles. From XRD results the best ratio of synthesis  $\text{SnO}_2\text{-Fe}_3\text{O}_4$  which has a mass ratio (1:2), which showed the highest intensity around the angle of  $2\theta = 26.74^\circ$  and  $34.08^\circ$ . Data from XRD characterization results and particle size calculations for  $\text{SnO}_2\text{-Fe}_3\text{O}_4$  using the Debye-Scherrer formula. From the calculation, obtained size of  $\text{SnO}_2\text{-Fe}_3\text{O}_4$  (1:1) is  $9.833$  nm,  $\text{SnO}_2\text{-Fe}_3\text{O}_4$  (1:2) is  $9.662$  nm and  $\text{SnO}_2\text{-Fe}_3\text{O}_4$  (2:1) is  $13.543$  nm, which shows that  $\text{SnO}_2\text{-Fe}_3\text{O}_4$  has a nanoparticle shape because it has a particle size of below  $100$  nm.

#### Characterization of $\text{SnO}_2\text{-Fe}_3\text{O}_4$ Nanocomposite using FTIR

The synthesized  $\text{SnO}_2\text{-Fe}_3\text{O}_4$  composite was also characterized using an FT-IR spectrophotometer. Spectrophotometry IR is one method that can be used to analyzed chemical compounds. This characterization aims to identify the functional group of the composite. The FT-IR spectrum is presented in Figure 5.

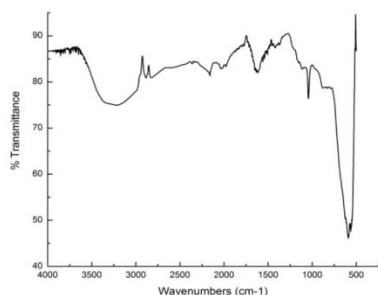


**Figure 5.** FT-IR analysis of  $\text{SnO}_2\text{-Fe}_3\text{O}_4$

The FT-IR spectra of the samples are shown in Figure 5. The broad absorption band observed at 3212 corresponds to the O-H stretching vibration of water molecules present at  $\text{SnO}_2\text{-Fe}_3\text{O}_4$ . The absorbance band at  $1632\text{ cm}^{-1}$  can be associated with the bending vibrations of asymmetrical  $\text{H}_2\text{O}$  molecules. The broad absorption peak appears between  $550\text{-}840\text{ cm}^{-1}$  are assigned to metal-oxygen (M-O). The absorption band at  $590\text{ cm}^{-1}$  is a characteristic peak of Sn-O stretching vibrations of  $\text{SnO}_2$  nanoplates. The absorption band at  $563\text{ cm}^{-1}$  corresponds to Fe-O stretching vibrations of the  $\text{Fe}_3\text{O}_4$  nanosphere [17].

#### Characterization of $\text{SnO}_2\text{-Fe}_3\text{O}_4$ Nanocomposite using TEM

The synthesized  $\text{SnO}_2\text{-Fe}_3\text{O}_4$  composite was also characterized using TEM. Figure 6 presents the typical transmission electron microscopy (TEM) images of  $\text{SnO}_2$ .

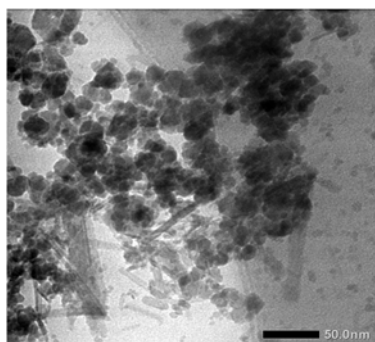


**Figure 6.** TEM images of  $\text{SnO}_2\text{-Fe}_3\text{O}_4$

Based on the TEM results, the morphological or structural results of the synthesis of  $\text{SnO}_2\text{-Fe}_3\text{O}_4$  were obtained. The nanocomposite has a structure in the form of aggregation or a unified structure. Based on the TEM image, there was a material morphology in the shape of a rod that has a flat hexagonal crystallographic plane, and it assumed as the shape of  $\text{SnO}_2$  [18]. From the TEM results, it can also be observed that there is an aggregated phase is

seen with a darker black color intensity at several points which shows the aggregation of  $\text{Fe}_3\text{O}_4$  particles [19].  $\text{Fe}_3\text{O}_4$  synthesized by co-precipitation indicated the mean size of the particle was 8 nm. The control of the monodisperse size is very important because the properties of the nanocrystal strongly depend upon the dimension of nanoparticles [20].

#### Nanocomposite Antibacterial Test Result

Antibacterial test was conducted to determine the ability of Nanocomposite  $\text{SnO}_2\text{-Fe}_3\text{O}_4$  to inhibit bacterial growth. Antibacterial  $\text{SnO}_2\text{-Fe}_3\text{O}_4$  nanocomposite test results on bacteria *Staphylococcus aureus* and *Escherichia coli* against both types of bacteria show the formation of a clear zone. This clear zone is a zone of inhibition which indicates that bacteria do not grow in the area. The results of the  $\text{SnO}_2\text{-Fe}_3\text{O}_4$  nanocomposite antibacterial test against *Staphylococcus aureus* and *Escherichia coli* are shown in Figure 7.

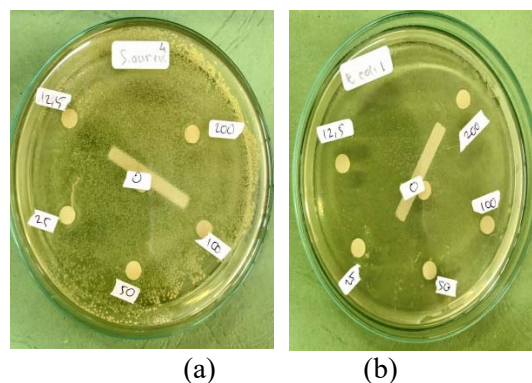


**Figure 7.** Antibacterial Test Results with various concentrations (a) *Staphylococcus aureus* (b) *Escherichia coli*

Based on Figure 7, it can be seen that the nanocomposite  $\text{SnO}_2\text{-Fe}_3\text{O}_4$  can inhibit the growth of both bacteria. From the observations, the concentration of nanocomposite  $\text{SnO}_2\text{-Fe}_3\text{O}_4$  can affect the diameter of the resulting inhibition zone. The higher the nanocomposite  $\text{SnO}_2\text{-Fe}_3\text{O}_4$  concentration used, the larger the inhibition zone formed. This is because the greater the concentration of nanocomposite  $\text{SnO}_2\text{-Fe}_3\text{O}_4$  used, the faster it will interact with bacteria, causing a larger diameter of the inhibition zone formed [21]. From the observation of the image above, the type of bacteria can affect the formed inhibition zone, where the results of the nanocomposite  $\text{SnO}_2\text{-Fe}_3\text{O}_4$  antibacterial test against *Staphylococcus aureus*

bacteria have a larger inhibition zone than the *Escherichia coli* bacteria, this is following previous studies [22]. Graph of nanocomposite SnO<sub>2</sub>-Fe<sub>3</sub>O<sub>4</sub> inhibition zone diameter against *Staphylococcus aureus* and *Escherichia coli* can be seen in Figure 8.

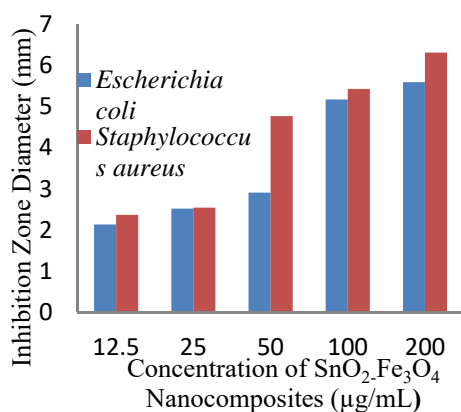


**Figure 8.** Inhibition Zone Diameter Graph of SnO<sub>2</sub>-Fe<sub>3</sub>O<sub>4</sub> nanocomposites

Based on Figure 8, it can be seen that the higher the concentration of antibacterial compounds, the greater the antibacterial activity produced. The Minimum Inhibitory Concentration (MIC) of nanocomposite SnO<sub>2</sub>-Fe<sub>3</sub>O<sub>4</sub> against *Staphylococcus aureus* and *Escherichia coli* was obtained at the same concentration of 12.5 µg/mL.

## CONCLUSION

Synthesis of SnO<sub>2</sub>-Fe<sub>3</sub>O<sub>4</sub> composites with mass ratio (1:1), (1:2) and (2:1) has been successful. The results of characterization using XRD showed the highest intensity around the angle of 2θ = 26.74° and 34.08°. Characterization SnO<sub>2</sub>-Fe<sub>3</sub>O<sub>4</sub> using FTIR showed the absorption band at 590 cm<sup>-1</sup> is a characteristic peak of Sn-O and the absorption band at 563 cm<sup>-1</sup> corresponds to Fe-O. From the TEM image, there was a material morphology in the shape of a rod that has a flat hexagonal crystallographic plane and has a structure in the form of aggregation. Nanocomposite SnO<sub>2</sub>-Fe<sub>3</sub>O<sub>4</sub> has antibacterial properties where the inhibition zone against *Staphylococcus aureus* is better than *Escherichia coli*.

## ACKNOWLEDGEMENT

We thank to DIKTI for the financial support of this research through Hibah Penelitian Penugasan WORLD CLASS RESEARCH 2020.

## REFERENCES

- [1] H.Q. Wu, S.F. Cao, X.W. Yin, X.W. Liu and X.R. Zhang. "Amino Acid-Assisted Hydrothermal Synthesis and Photocatalysts of SnO<sub>2</sub> Nanocrystals." *The Journal of Physical Chemistry C*, vol. 113, no. 41, pp.13-18, 2009.
- [2] S. Bharati, D. Nataraj, D. Mangalaraj, Y. Masuda, K. Senthil, and K. Yong. "Highly Mesoporous α-Fe<sub>2</sub>O<sub>3</sub> Nanostructures: Preparation: Characterization and Improved Photocatalytic Performance Toward Rhodamine B." *Journal of Physics D: Applied Physics*, vol 43, pp. 1-9, 2010.
- [3] H.E. Gandhoor, H.M. Zidan, M.H.K. Mostafa, and M.I.M. Ismail, "Synthesis and Some Physical Properties Magnetite (Fe<sub>3</sub>O<sub>4</sub>) Nanoparticles." *International Journal of Electrochemical Science*, vol 7, pp. 5734-5745, 2012.
- [4], V.S. Kundu, R.L. Diman, D. Singh, A.S. Maan, and S. Arora, "Synthesis and Characterization of Tin Oxide Nanoparticles Via Sol-Gel Method Using Ethanol as Solvent." *International Journal of Advanced Research in Science And Engineering*, vol. 2, no. 1, pp. 1-5, 2013.
- [5] H. Widiyandari, A. Purwanto, V. Gunawan, and S.A. Widyanto, "Synthesis of Titanium Dioxide (TiO<sub>2</sub>) Fine Particle by Flame Spray Pyrolysis (FSP) Method Using Liquid Petroleum Gas (LPG) as Fuel." *Chemical Engineering Journal*, vol. 17, no. 4, pp. 1-12, 2017.
- [6] Y. Liang, and B. Fang, "Hydrothermal Synthesis of SnO<sub>2</sub> Nanorods: Morphology Dependence, Growth Mechanism and Surface Properties." *Materials Research Bulletin*, vol. 48, no. 10, pp. 4118-4124, 2013.
- [7] G.T. Zhu, X.L. Hu, X.M. He, S.K. Zhu, and Y.Q. Feng, "Hydrothermally Tailor-made Chitosan Fiber for Micro-solid Phase Extraction of Petroleum Acids in Crude Oils." *Journal of Chromatography*, vol. 1564, pp. 42-50, 2018.
- [8] P. Bothakur, and M.R. Das, "Hydrothermal Assisted Decoration of NiS<sub>2</sub> and CoS Nanoparticles on the Reduced Graphene Oxide Nano sheets for Sunlight Driven Photocatalytic Degradation of Azo Dye: Effect of Background Electrolyte and Surface Charge." *Journal of Colloid and Interface Science*, vol. 516, pp. 342-352, 2018.

- [9] W.W. Wang, and Yao, J.L., "Hydrothermal Synthesis of SnO<sub>2</sub>/Fe<sub>3</sub>O<sub>4</sub> Nanocomposites and Their Magnetic Property." *J. Phys. Chem*, vol. 113, no.8, pp. 3070-3075, 2009.
- [10] A.S. Buteica, D.E. Mihaiescu, A. M. Grumezescu, B. Ş. Vasile, A. Popescu, M. Mihaiescu, and R. Cristescu, "The Anti-Bacterial Activity Of Magnetic Nanofluid: Fe<sub>3</sub>O<sub>4</sub>/OleicAcid/CephalosporinsCore/Shell/ Adsorptionshell Proved on S. Aureus and E. Coli and Possible Applications as Drug Delivery Systems." *Digest Journal of Nanomaterials and Biostructures*, vol. 5, no. 4, pp. 927-932, 2010.
- [11] A. Huda, R. Ichwani, C.T. Handoko, B. Yudono, M.D. Bustan, and F. Gulo, "Enhancing The Visible-light Photoresponse of SnO<sub>2</sub> and SnO<sub>2</sub> through The Heterogenous Formation Using One-Step Hydrothermal Route." *Materials Letters*, pp. 1-8, 2018.
- [12] A. Ayeshamariam, A. Vidya, S. Sivaranjani, M. Bououdina, R. Perumalsamy, and M. Jayachandran, "Synthesis and Characterizations of SnO<sub>2</sub> Nanoparticles." *Journal of Nanoelectronics and Optoelectronics*, vol. 8, no. 1-8, pp. 1-8, 2013.
- [13] P.L. Hariani F. Faizal, M. Ridwan, and D. Setiabudidaya, "Synthesis and Properties of Fe<sub>3</sub>O<sub>4</sub> Nanoparticles by Co-precipitation Method to Removal Precion Dye." *International Journal of Enviromental Science and Development*, vol. 4, no. 3, pp. 336-340, 2013.
- [14] R. Liu, Y. Zhao, R. Huang, Y. Zhao, and H Zhou, "Phase Transformation and Shape Evolution of Iron Oxide Nanocrystal Synthesized in the Ethylene Glycol-Water System, Science China Physics." *Mechanics and Astronomy*, vol. 54, no. 7, pp. 1271-1276, 2011.
- [15] X.M. Li, G. Xu, Y. Liu, and T. He, "Magnetic Fe<sub>3</sub>O<sub>4</sub> Nanoparticles: Synthesis and Application in Water Treatment." *Nanoscience & Nanotechnology-Asia*, vol. 1, no. 1, pp. 14-24, 2012.
- [16] W.W. Wang, , and J.L. Yao, "Hydrothermal Synthesis of SnO<sub>2</sub>/Fe<sub>3</sub>O<sub>4</sub> Nanocomposites and Their Magnetic Property." *J. Phys. Chem*, vol. 113, no. 8, pp. 3070-3075, 2009.
- [17] V.M. Vinosel, S. Anand, M.A.Janifer, S. Pauline, S. Dhanavel, P. Praveena, A. Stephen, "Enhanced Photocatalytic Activity of Fe<sub>3</sub>O<sub>4</sub>/SnO<sub>2</sub> magnetic Nanocomposite for the Degradation of Organic Dye." *Journal of Materials Science Materials*, vol. 1, no. 1, pp. 1-16, 2019.
- [18] J. Huang, X. Xu, , C. Gu, S. Yao, Y. Sun and J. Liu, "Large-scale Selective Preparation of Porous SnO<sub>2</sub> 3D architecture and Their Gas-sensing Property," *Cryst. Eng. Comm*, vol. 14, pp. 3283-3290, 2012.
- [19] F. Wang, J. Liu, X. Wang, J. Kong, and S. Qiu, "Synthesis of Hollow at ZnO at Anatase TiO<sub>2</sub> Core-shell Structured Spheres." *Ceramics International*, vol. 38, no. 1, pp. 6899-6902, 2012.
- [20] L. Sophie, F. Delphine, R. Marc, R. Alain, V.E. Caroline, Luce and N.M. Robert, "Magnetic Iron Oxide Nanoparticles: Synthesis, Stabilization, Vectorization, Physicochemical Characterization, and Biological Application." *Chem. Rev.*, vol. 108, pp. 2064-2110, 2008.
- [21] S.M. Amininezhad, A. Rezvani, M. Amouheidari, and Aminnejad, S.M, "The Antibacterial Activity of SnO<sub>2</sub> Nanoparticles against *Escherichia coli* and *Staphylococcus aureus*." *Res. Med. Sci*, vol. 17, no. 9, pp. 1-5, 2015.
- [22] N. John, M. Somaraj, N.J. Tharayil, "Synthesis, Characterization and Anti – Bacterial Activities of SnO<sub>2</sub> Nanoparticles Using Biological Molecule." *Materials Science and Engineering*, vol. 360, pp. 1-11, 2018.